JOURNAL OF MATERIALS SCIENCE 28 (1993) 4421–4426

Effect of rigid inclusions on the sintering of mullite synthesized by sol–gel processing

D.-Y. JENG*, M. N. RAHAMAN
University of Missouri-Rolla, Ceramic Engineering Department, Rolla, MO 65401, USA

The effect of crystalline particulate inclusions of mullite or zirconia on the sintering and crystallization of a mullite powder matrix was investigated as a function of the inclusion volume fraction and size. The mullite powder was synthesized by sol–gel processing and, within the limits of X-ray diffraction, was amorphous. Composites containing up to 22.5 vol % zirconia reached almost full density after sintering at 1500 °C for 1 h. Under identical conditions, the sintered density of the composites containing crystalline mullite inclusions was considerably lower. The zirconia inclusions were inert but the mullite inclusions enhanced the independent nucleation and growth rate of the mullite crystals in the matrix. The lower sintering rate of the matrix reinforced with crystalline mullite is attributed to the enhanced matrix crystallization.

1. Introduction

Ceramic matrix composites are required to meet the demands of many technological applications ranging from advanced heat engines to electronic substrates. The most recognized path to the formation of polycrystalline ceramics involves powder compaction into a porous body that is made dense by heat treatment. In the formation of polycrystalline matrix composites however, the presence of second-phase inclusions (e.g. particles, whiskers or fibres) leads to a drastic reduction in the matrix densification rate. Thus considerable difficulties are often encountered in the formation of polycrystalline matrix composites by conventional, pressureless sintering. While techniques such as hot pressing and hot isostatic pressing are effective for fabricating composites with high density, they may have severe limitations for a number of applications. It will be useful, therefore, to explore techniques that have the potential for producing high-density composites by pressureless sintering.

As outlined earlier [1], densification prior to crystallization (i.e. a glass-ceramic route) is expected to be particularly important for forming high-density composites by conventional pressureless sintering. At an equivalent inclusion content, glass matrices have been shown to exhibit a much higher sinterability compared to polycrystalline matrices [2–7]. The aim of the glass-ceramic route is to exploit the beneficial sintering characteristics of amorphous (or glass) matrices. After densification, it will be necessary to control the crystallization of the matrix to obtain the required microstructure.

The sintering and crystallization of a mullite powder synthesized by sol–gel processing has been reported in an earlier paper [1]. Within the limits of detection by X-ray analysis, the synthesized powder was amorphous. The compacted powder densified appreciably prior to the onset of crystallization and was therefore considered to be a good model powder for investigating the usefulness of the glass-ceramic route for the formation of dense composites by conventional sintering.

In the work reported in the present paper, the effect of rigid particulate inclusions on the sinterability of the mullite powder was investigated. Crystalline inclusions of two different compositions were used: zirconia and mullite. For the sintering temperatures employed, the zirconia inclusions were expected to be inert, while the crystalline mullite inclusions were expected to enhance the independent nucleation and growth rate for the crystallization of the matrix phase. The effects of inclusion size and volume fraction on the sintering and crystallization of the matrix were investigated.

2. Experimental procedure

Mullite powder, synthesized by a sol–gel route described earlier [1], was used as the matrix phase in the formation of the composites. The composition of the powder corresponded to that for stoichiometric mullite ($3Al_2O_3 \cdot 2SiO_2$) and, within the limits of X-ray diffraction, was amorphous. Crystalline zirconia (Grade SC; Magnesium Electron, Flemington, NJ, USA) with an average size of 2.5 μm and crystalline mullite (Catapal XM; Vista Chemical Company, Houston, TX, USA) with two different average sizes of 0.3 and 2 μm, were used as the particulate inclusion phase. The inclusions were heated at 1600 °C for 1 h to densify any agglomerates and then milled prior to incorporation into the matrix phase.

Composites containing 0, 7.5, 15, and 22.5 vol % inclusion phase were formed by conventional techniques. The matrix powder and the inclusion phase were mixed in isopropanol, stir dried, and then ground

Present address: Department of Materials Science and Engineering, University of California, Los Angeles, CA 90024, USA.

0022–2461

lightly in an agate mortar and pestle to break up agglomerates. For comparison, the unreinforced mullite powder was subjected to the same mixing treatment. The unreinforced and composite powders were pressed uniaxially in a die at $\approx$ 10 MPa pressure followed by isostatic pressing at $\approx$ 280 MPa to form green compacts (6 mm diameter by 5 mm) for subsequent sintering experiments. It was found difficult to compact the unreinforced mullite powder to densities greater than $\approx$ 0.50, but the composites were easier to compact. In the experiments, the green density of the unreinforced mullite was 0.48 $\pm$ 0.02 while the values for the composites were 0.56 $\pm$ 0.02.

Sintering was performed in air in a dilatometer that allowed continuous monitoring of the axial shrinkage (Theta Industries Inc., Port Washington, NY, USA). The compacts were heated at a constant rate of 5 °C min^{-1} to 1500 °C and then held at this temperature for 1 h. The density of the samples at any temperature (or time) was measured from the mass and dimensions and the final density was compared with the value measured by Archimedes' principle.

X-ray diffraction was used to study the crystallization of the mullite matrix and the possibility of interfacial reaction between the matrix and the inclusion phase during sintering. For these studies, samples containing 0 and 15 vol % inclusion phase were used. The samples were sintered at 5 °C to the appropriate temperature and then cooled rapidly to room temperature. The sintered samples were crushed and ground into a fine powder in an agate mortar and pestle. A fixed amount of MgO (20 wt %) was mixed with the powder and used as an internal standard. The X-ray diffraction patterns were obtained using CuK_α radiation at a scanning rate of 1° 2Θ min^{-1}. The relative matrix crystallinity in the samples was determined by an internal standard analysis [8], using the strongest mullite peak in the X-ray pattern. The peak areas were taken to be proportional to the product of the half-width and the height above the background.

The microstructures of the sintered samples were observed by scanning electron microscopy of fractured and polished surfaces. The preparation technique for the polished surfaces was identical to that described in the preceding paper [1].

3. Results

3.1. Sintering of the composites

Fig. 1 shows the data for the axial shrinkage, $\Delta L/L_0$, versus temperature for the mullite powder matrix containing 0, 7.5, 15, and 22.5 vol % ZrO_2 inclusions (L_0 = initial sample length, $\Delta L = L - L_0$, where L is the instantaneous sample length). Each curve is the average of two runs under the same conditions and the data at any temperature are reproducible to $\pm$ 0.01. Most of the shrinkage occurs below $\approx$ 1250 °C. This temperature has been shown earlier [1] to correspond approximately to the onset of crystallization of the amorphous mullite powder. At any temperature, the shrinkage decreases with increasing volume fraction of inclusions. Above $\approx$ 1250 °C, the unreinforced sample shows almost no further shrinkage; however, the

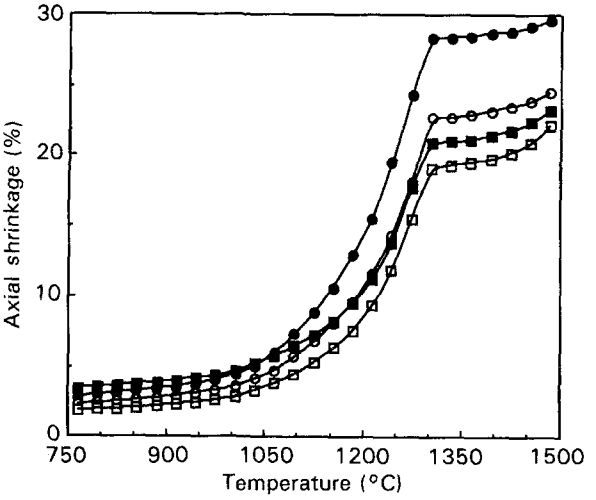

Figure 1 Axial shrinkage versus temperature for the mullite powder matrix containing ZrO_2 inclusions (2.5 μm) for sintering at 5 °C min^{-1} to 1500 °C, followed by a holding time of 1 h. (●) 0 vol %, (○) 7.5 vol %, (■) 15 vol %, (□) 22.5 vol %.

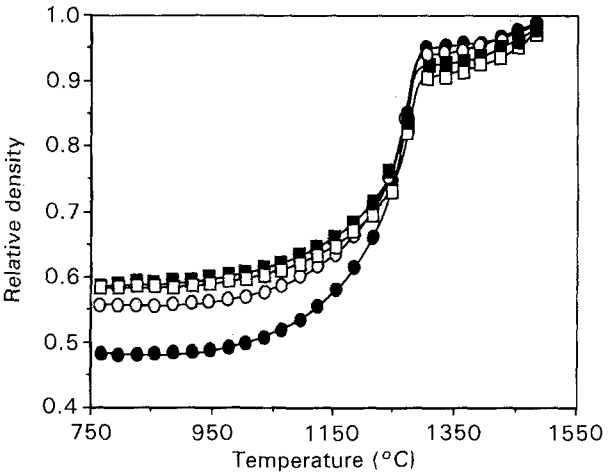

Figure 2 Relative density versus temperature for the samples described in Fig. 1.

shrinkage of the composite samples increases slightly above this temperature, with the overall magnitude of the increase being higher for the samples with higher inclusion content.

The relative density of the samples was calculated from the data of Fig. 1 and the results are shown as a function of temperature in Fig. 2. As outlined earlier, the unreinforced mullite powder did not compact as well as the composite powder and the initial density of the green bodies was $\approx$ 0.48 (expressed as a fraction of the theoretical density). Nevertheless, the unreinforced samples reached nearly full density ($\approx$ 0.97) after sintering. The initial density of the composite samples was in a narrow range of 0.56–0.58 and the sintered density shows no significant dependence on the inclusion content. At the end of the sintering process, all of the composite samples reached a density of $\approx$ 0.97. This is in sharp contrast to polycrystalline ceramic matrices, where a rigid inclusion phase leads to a drastic reduction in the densification rate [4–6].

Fig. 3 shows the data for $\Delta L/L_0$ versus temperature for the mullite matrix containing crystalline mullite

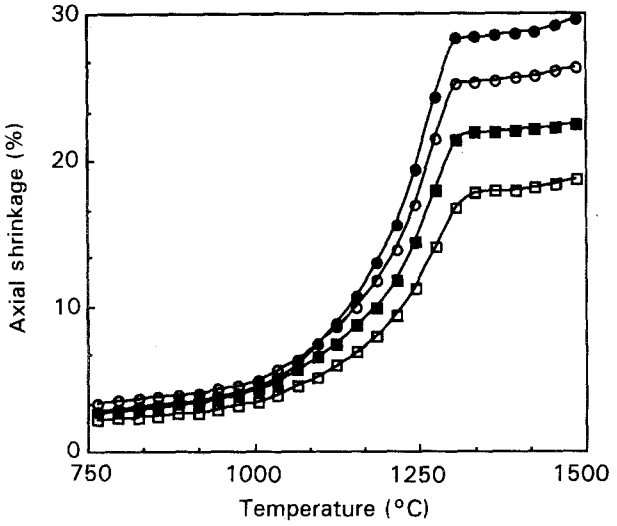

Figure 3 Axial shrinkage versus temperature for the mullite powder matrix containing crystalline mullite inclusions (0.3 μm) for the same sintering conditions described in Fig. 1.

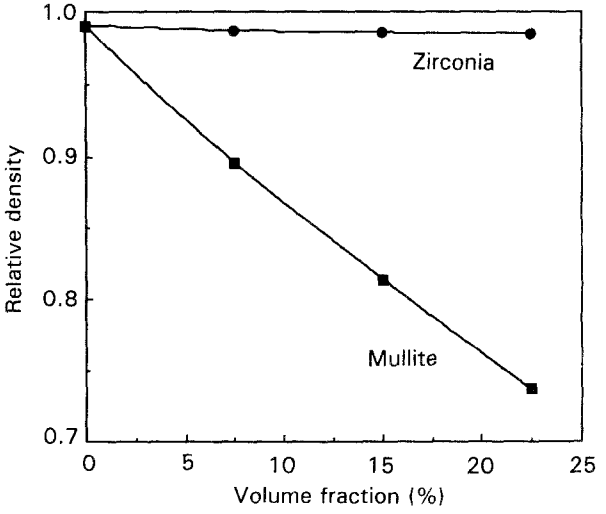

Figure 5 Final sintered density versus inclusion volume fraction for the composites containing ZrO_2 or crystalline mullite inclusions.

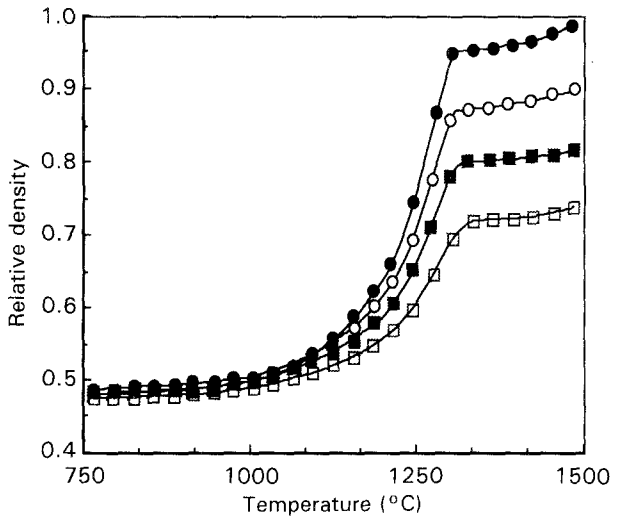

Figure 4 Relative density versus temperature for the samples described in Fig. 3. For key, see Fig. 1.

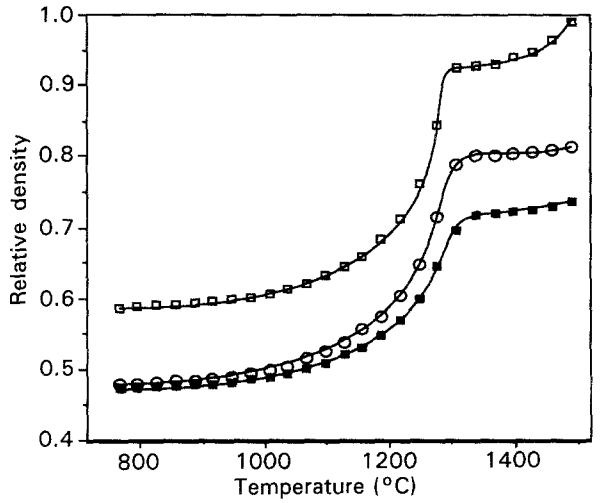

Figure 6 Relative density versus temperature for the composites containing 15 vol % inclusions of (□) ZrO_2 (2.5 μm), (○) "coarse" mullite (2 μm), or (■) "fine" mullite (0.3 μm).

inclusions (particle size 0.3 μm). Compared to the data of Fig. 1 for the ZrO_2 inclusions, the curves have similar shapes but the shrinkage decreases more appreciably with increasing inclusion content. The density of the mullite-reinforced samples (calculated from the data of Fig. 3) are shown as a function of temperature in Fig. 4. At any temperature, the density decreases significantly with increasing volume fraction of the inclusions. The magnitude of this decrease is much higher than that observed for the ZrO_2 inclusions (Fig. 2).

The final density of the composites (i.e. after sintering at 5 °C min^{-1} to 1500 °C and holding at this temperature for 1 h) plotted as a function of the inclusion content for the ZrO_2 and the mullite inclusions is shown in Fig. 5. It is seen that the composites containing the ZrO_2 inclusions sinter to almost full density for the range of inclusion contents investigated (i.e. up to 22.5 vol %). In contrast, the density of the samples containing the mullite inclusions decreases significantly with increasing inclusion content.

Fig. 6 shows data for the relative density versus temperature for the composites containing 15 vol % inclusions of ZrO_2 (average size $\approx$ 2.5 μm), "coarse" mullite ($\approx$ 2 μm), and "fine" mullite ($\approx$ 0.3 μm). It is seen that for an equivalent inclusion volume fraction and for an approximately equivalent inclusion size, the sinterability of the mullite-reinforced composites decrease considerably compared with the ZrO_2-reinforced composites. Furthermore, for an equivalent inclusion content, the sinterability of the mullite-reinforced composites decreases with decrease in the inclusion size.

3.2. Microstructural observations

Fig. 7 shows scanning electron micrographs of (a) the fracture surface of the sintered composite containing 15 vol % ZrO_2 inclusions, and (b) a polished surface of a sintered composite containing 15 vol % crystalline inclusions (size 0.3 μm). The samples were sintered at 1500 °C for 1 h and the final densities of those shown

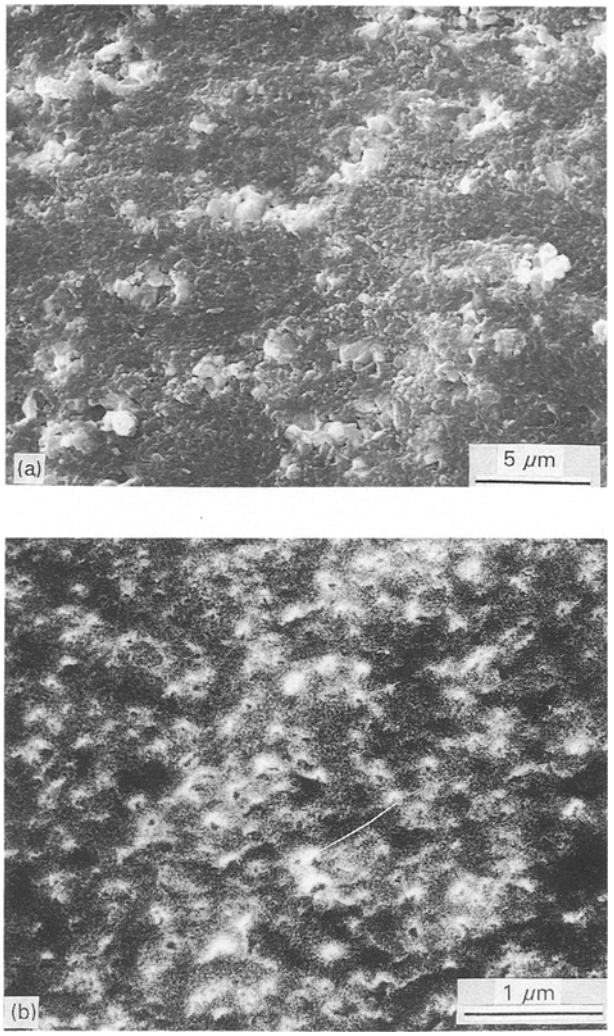

Figure 7 Scanning electron micrographs of (a) a fracture surface of a composite containing 15 vol % ZrO_2 inclusions (2.5 μm), and (b) a polished surface of a composite containing 15 vol % mullite inclusions (0.3 μm). The relative densities of the samples shown in (a) and (b) were 0.97 and 0.85, respectively.

in Fig. 7a and b were 0.97 and 0.85, respectively. The zirconia inclusions are somewhat agglomerated and minor traces of porosity are present within the agglomerated inclusions. The presence of porosity within the inclusion agglomerates may account for some of the residual porosity in the sintered sample. For the sample containing the mullite inclusions, the micrograph shows a large number of fine pores distributed fairly uniformly within the body.

3.3. X-ray analysis

Fig. 8 shows the X-ray diffraction pattern of a composite containing 15 vol % ZrO_2 inclusions after the sample was sintered at 1500 °C for 1 h. The pattern consists of mullite and ZrO_2 peaks only. Thus, within the limits of detectability of the instrument (less than ± 1%), there was no reaction between the mullite matrix and the ZrO_2 inclusions.

As outlined earlier, it is highly likely that the crystalline mullite inclusions can influence the independent nucleation and growth rate of the matrix crystals. The effect of the inclusion phase on the matrix crystallization was studied by X-ray analysis of partially sintered composites. Fig. 9 shows the integrated peak intensity of the main mullite peak relative to that for the MgO standard, I_{Mul}/I_{MgO}, for the unreinforced mullite and composites containing 15 vol % mullite inclusions (size ≈ 2 or 0.3 μm). The samples were sintered at 5 °C min^{-1} to 1200 °C. If the mullite inclusions had no effect on the growth rate of the mullite crystals in the matrix, then the I_{Mul}/I_{MgO} ratio would be expected to be the same for the two composites. The significantly higher ratio for the sample with the smaller inclusions therefore indicate that the mullite inclusions are indeed causing an enhancement of the independent nucleation and growth rate in the bulk of the matrix.

4. Discussion

For the amorphous mullite powder matrix containing ZrO_2 inclusions, the X-ray diffaction data of Fig. 8 showed no reaction between the matrix phase and the inclusions. The inclusions can therefore be considered to be inert and rigid. In this case, the composites containing up to 22.5 vol % inclusions reached almost full density after sintering at 1500 °C for 1 h. Earlier work [1] had shown that the microstructure of the unreinforced mullite consisted of nearly equiaxed grains with an average size of 0.2 μm after sintering under the same conditions. In the case of the inert ZrO_2 inclusions which do not affect the independent nucleation and growth of the matrix crystals, the composite matrix would be expected to have a microstructure similar to that observed for the unreinforced mullite.

The formation of nearly fully dense ZrO_2 reinforced mullite by the "glass-ceramic" route used in the present work would appear to be a significant improvement over conventional routes which employ crystalline mullite as the starting powder. Normally, powder compacts of unreinforced crystalline mullite (particle size ≈ 1 μm) must be sintered for a few hours at temperatures above 1600 °C in order to achieve near theoretical density [9]. Recent studies [10–12] indicate that the incorporation of coarse, inert rigid inclusions into the crystalline mullite matrix would decrease the sinterability significantly.

In the case of the "amorphous" mullite powder matrix containing crystalline mullite inclusions, the sinterability of the matrix is reduced significantly compared to the same matrix containing ZrO_2 inclusions. One factor that can contribute to the reduced sinterability of the matrix is the enhanced crystallization of the matrix due to the presence of the mullite inclusions (Fig. 9). Morz and Laughner [13] have also shown that the addition of crystalline mullite to mullite gels yielded distinct changes in the fired microstructure. The increased crystallinity of the mullite-reinforced sample may occur by a mechanism of growth on existing nuclei at the inclusion–matrix boundary [14]. The growth of the inclusion phase into the matrix is controlled either by the interfacial reaction or short-range diffusion near the surface. In either case, the enhanced crystallization would be dependent on the inclusion surface area. This is indeed found to be so (Fig. 9).

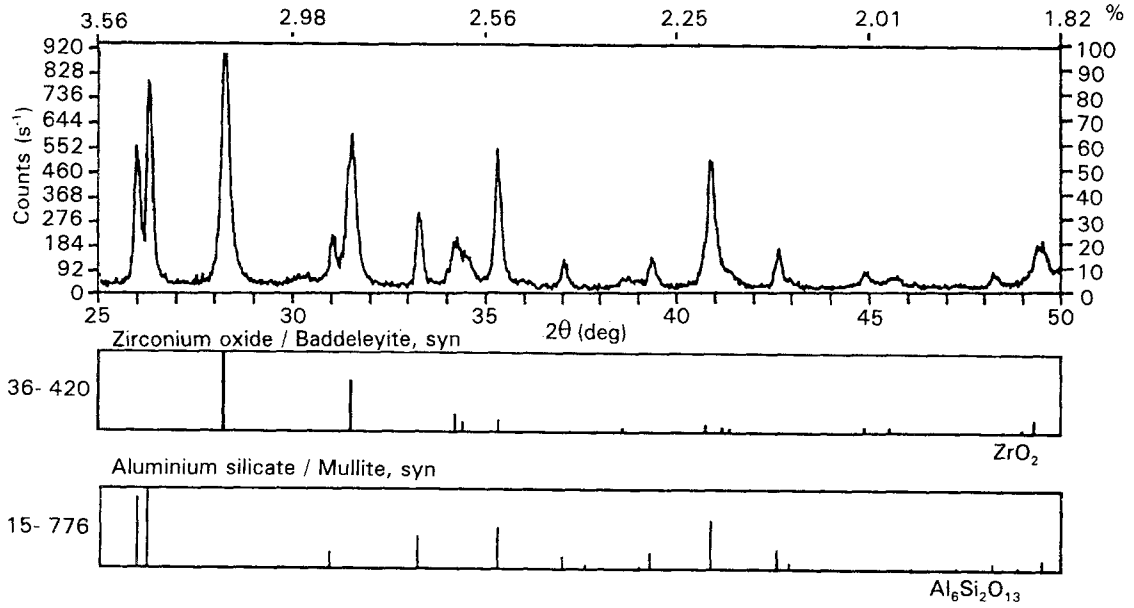

Figure 8 X-ray diffraction pattern of a composite containing 15 vol % ZrO_2 inclusions after sintering at 1500 °C for 1 h. For comparison, the reference peaks of mullite and ZrO_2 are also shown.

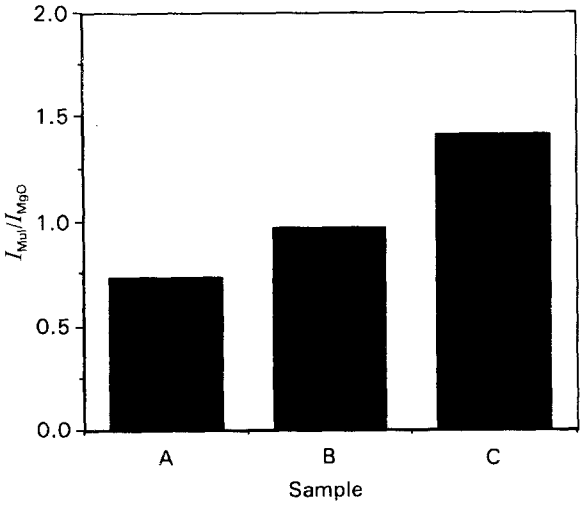

Figure 9 Integrated mullite peak intensity relative to the MgO standard, for the unreinforced mullite (A), and the composites containing 15 vol % 2 μm mullite inclusions (B), and of 0.3 μm mullite inclusions (C). The samples were sintered at 5°C min^{-1} to 1200°C.

The growth of the mullite inclusions into the matrix may influence the sintering of the body in two ways mainly. First, the growth of the inclusions may be considered to lead to an increase in the effective volume fraction of the inclusion phase. Considering a powder compact with a volume V_0, containing an initial volume fraction of inclusions, f_i, with a radius R, if the inclusions grow during sintering to a radius $R + t$, where t is the thickness of the induced crystallization zone, then the initial and the effective volume fraction, f_e, of the inclusions are related by

$$V_0 f_i = N(4/3)\pi R^3 \quad (1)$$

and

$$V_0 f_e = N(4/3)\pi(R + t)^3 \quad (2)$$

where N is the number of inclusions. Therefore

$$f_e = f_i(1 + t/R)^3 \quad (3)$$

According to Equation 3, f_e increases as the inclusion size, R, decreases for a constant value of t. Second, the increase in f_e would be expected to lead to an increase in the composite viscosity. According to Bordia and Scherer's self-consistent model for sintering with rigid inclusions [10], the densification rate of the composite, $\dot{\varepsilon}_c$, relative to that for the unconstrained (or free) matrix, $\dot{\varepsilon}_{fm}$, is given by

$$\dot{\varepsilon}/\dot{\varepsilon}_{fm} = (1 - f)/[1 + f(4G_c)/(3K_m)] \quad (4)$$

where f is the inclusion volume fraction, G_c is the shear viscosity of the composite, and K_m is the bulk viscosity of the matrix phase. An increase in both f and G_c would therefore be expected to lead to a significant reduction in the densification of the composite compared to the unreinforced mullite (Fig. 5).

5. Conclusions

1. The sintering and crystallization of an amorphous mullite powder (prepared by sol–gel processing) were influenced significantly by the chemical composition of the reinforcement phase (crystalline mullite or ZrO_2 inclusions).

2. The ZrO_2 inclusions were inert toward the matrix at the sintering temperatures used and had a much smaller effect on the composite densification rate compared to the crystalline mullite inclusions. Composites containing up to 22.5 vol % ZrO_2 inclusions reached nearly full density after sintering for 1 h at 1500 °C.

3. The crystalline mullite inclusions enhanced the independent nucleation and growth rate of the mullite crystals in the matrix phase and caused a significant reduction in the composite densification rate.

4. The decreased densification rate of the composites containing the crystalline mullite inclusions is consistent with a mechanism involving the growth of the mullite inclusions into the matrix.

References

1. D.-Y. JENG and M. N. RAHAMAN, *J. Mater. Sci.*
2. R. RAJ and R. K. BORDIA, *Acta Metall.* **32** (1984) 1003.
3. C. H. HSUEH, A. G. EVANS, R. M. CANNON and R. J. BROOK, *ibid.* **34** (1986) 927.
4. L. C. DE JONGHE, M. N. RAHAMAN and C-H. HSUEH, *ibid.* **34** (1986) 1467.
5. R. K. BORDIA and R. RAJ, *J. Am. Ceram. Soc.* **71** (1988) 302.
6. W. H. TUAN, E. GILBART, and R. J. BROOK, *J. Mater. Sci.* **24** (1989) 1062.
7. M. N. RAHAMAN and L. C. DE JONGHE, *J. Am. Ceram. Soc.* **70** (1987) C-348.
8. H. P. KLUG and L. E. ALEXANDER, "X-Ray Diffraction Procedures", 2nd edn (Wiley, New York, 1974) p. 549.
9. B. L. METCALF and J. H. SANT, *Trans. J. Brit. Ceram. Soc.* **74** (1975) 193.
10. R. K. BORDIA and G. W. SCHERER, *Acta Metall.* **36** (1988) 2411.
11. G. W. SCHERER, *J. Am. Ceram. Soc.* **70** (1987) 719.
12. L. C. DE JONGHE and M. N. RAHAMAN, *Acta Metall.* **36** (1988) 223.
13. T. J. MORZ and J. W. LAUGHNER, *J. Am. Ceram. Soc.* **71** (1989) 508.
14. W. C. WEI and J. W. HALLORAN, *ibid.* **71** (1988) 581.

Received 13 March 1992
and accepted 11 January 1993